| | |
|---|---|
| Title | Coupled cantilever array with tunable on-site nonlinearity and observation of localized oscillations |
| Author(s) | Kimura, Masayuki; Hikihara, Takashi |
| Citation | Physics Letters A (2009), 373(14): 1257-1260 |
| Issue Date | 2009-03-23 |
| URL | http://hdl.handle.net/2433/123371 |
| Right | Copyright © 2009 Elsevier B.V. |
| Type | Journal Article |
| Textversion | author |

# Coupled Cantilever Array with Tunable On-site Nonlinearity and Observation of Localized Oscillations

Masayuki Kimura [a], Takashi Hikihara [a]

[a] *Department of Electrical Engineering, Kyoto University, Nishikyo, Kyoto 615-8510 Japan*

**Abstract**

A macro-mechanical cantilever array is newly proposed for experimental investigations of intrinsic localized mode (ILM). There has never reported such a macro-system which show ILMs mechanically. The array consists of cantilevers, electromagnets faced on the cantilevers, elastic rods for coupling between cantilevers, and a voice coil motor for external excitation. Nonlinearity appears in the magnetic interaction, that is, the restoring force of cantilever. Therefore it is tunable. In the array, ILMs are experimentally generated by the sinusoidal forced excitation. Observed ILMs are also identified in the model equation for the array.

*Key words:* Intrinsic localized mode, Discrete breather, Coupled cantilever array

*PACS:* 05.45.-a

## 1 Introduction

Energy localization phenomena are known as soliton for continuum media and intrinsic localized mode (ILM) for discrete media [1]. ILM, also called discrete breather (DB), appears as a spatially localized and temporally periodic solution in coupled differential equations with nonlinearity. ILM has been studied for various nonlinear coupled oscillators since it was analytically discovered by Sievers and Takeno [2]. Experimental observations have been appeared in this decade. ILM is identified in Josephson-junction arrays [3–5], optic wave guides [6,7], photonic crystals [8], micro-mechanical cantilever array [9], mixed-valence transition metal complexes [10,11], antiferromagnets [12], and electronic circuits [13]. These experiments directly suggest the phenomenological universality of ILM. In addition, it is expected to apply ILM to micro- or nano-devices for sensing and actuating applications because of scale in length of the experimental systems. In particular, cantilever structures are widely used in microscopic devices [14]. Then ILM in a micro-cantilever array has a potential to be utilized for sensors and actuators which have high sensitivity and accuracy.

To realize such applications, detail dynamical behaviors of ILM has to be investigated. Moreover, a control scheme is necessary, especially for actuating applications. That is, ILM has to be generated, moved, and destroyed as desired. A manipulation involving position control for ILM has been realized by M. Sato [15,16]. In the research, ILM is manipulated in a micro-cantilever array by a localized impurity. Therefore, the position of ILM can be controlled dynamically by adding an impurity.

To establish the control scheme, it is necessary to clarify a mechanism of the manipulation. In addition, experimental investigations are needed to confirm the clarified mechanism. For the purpose, the macro-system is useful to confirm the dynamics and the principles of the control method. Then a macro-system is proposed as an analogous dynamical model to the micro- or nano-system, so that the dynamical behaviors can be discussed experimentally.

One of the good analogous models is a magneto-elastic beam system [17–19]. The experimental model has a similar equation of motion to the micro-cantilever array in which ILMs were observed. In the model, permanent magnets are placed to adjust the on-site nonlinearity. If the magnetic field is adjustable at each site, it will be possible to add on release an impurity. So we designed a macro-mechanical cantilever array having tunable electro-magnets based on the magneto-elastic beam system. In this letter, we are going to show a model of the macro-mechanical cantilever array to investigate the micro-cantilever array fabricated by M. Sato. In the system, ILMs are experimentally observed and the existence is also confirmed in the numerical simulations of model. Through the experiments and numerical simulation, it becomes possible to discuss the method of controlling ILMs for future applications.

## 2 Macro-mechanical cantilever array

A schematic configuration of the macro-mechanical cantilever array is shown in Fig. 1. Eight cantilevers are arranged with an equal interval in one dimension. Size of the array are shown in Table 1. As shown in Fig. 1, each cantilever has a permanent magnet (PM) at its apex. An electromagnet (EM) is placed

below the PM with an appropriate gap. The magnetic force between the PM and the EM can approximately be described by Coulomb's law for magnetic charges. The interaction force shows nonlinear relationship to the displacement of cantilever. The configuration of magnetic charges is shown in Fig. 1(c). If the displacement of cantilever is sufficiently small relative to the length of cantilever, Coulomb's law for magnetic charges gives the force

$$\begin{aligned} F(u_n) =& \frac{m_{\mathrm{p}} m_{\mathrm{e}}}{4\pi\mu_0} \frac{u_n}{(u_n^2 + d_0^2)^{\frac{3}{2}}} \\ =& \chi(I_{\mathrm{EM}}) \frac{u_n}{(u_n^2 + d_0^2)^{\frac{3}{2}}}, \end{aligned} \tag{1}$$

where $m_{\mathrm{p}}$ and $m_{\mathrm{e}}$ correspond to the magnetic charge of PM and EM, respectively. The distance between PM and EM is denoted by $d_0$ at the equilibrium state. The magnetic permeability is represented by $\mu_0$. Because the magnitude of $m_{\mathrm{e}}$ depends on the current flowing in the EM, the interaction coefficient $\chi(I_{\mathrm{EM}})$ can be represented as a function of current. In this letter, we assume the linear relationship $\chi(I_{\mathrm{EM}}) = \chi_0 + \chi_1 I_{\mathrm{EM}}$. Because an EM has a ferromagnetic core, a force acting between PM and EM is attractive even if the current is kept to be zero. Thus $\chi_0$ is always negative. On the other hand, the current direction decides the sign of $\chi_1 I_{\mathrm{EM}}$. We choose the current enhancing the attractive force is positive, so that $\chi_1$ is also negative.

As for a small vibration of a single cantilever, the Euler-Bernoulli beam theory can be applied when the cantilever is thin in thickness. The partial differential equation gives the relationship between spatial modes and temporal frequencies. However, we are going to focus on the first mode at which amplitude at the tip is the largest in the cantilever. The frequency of the first mode is the lowest resonant frequency of the cantilever. At the first mode oscillation, motion of the tip is depicted by an ordinary differential equation. The motion

of the tip is equivalent to a spring-mass system having a natural frequency, $\omega_0$, which corresponds to the first mode frequency.

The coupling rod causes a coupling force depending on the difference of displacement of adjacent cantilevers. The force linearly changes against the difference of displacement if the deformation of the rod is sufficiently small. As shown in Fig. 1(a), the rod is attached near the support. The displacement of cantilever at the rod is quite small relative to the amplitude of tip vibration. Thus we can assume the linearity of the coupling force. Therefore, the equation of motion of the coupled cantilever array is depicted as follows:

$$\begin{aligned} \ddot{u}_n = & -\omega_0^2 u_n - \gamma \dot{u}_n + F(u_n) + A\cos(\omega t) \\ & - C(u_n - u_{n+1}) - C(u_n - u_{n-1}), \\ & n \in \{1, \ldots, 8\}, \end{aligned} \tag{2}$$

where $\gamma$ denotes a damping coefficient of each cantilever. The fourth term in the right hand side of Eq. (2) represents the time-periodic external force excited by the voice coil motor. Both ends of array are fixed. Then the boundary conditions are given by,

$$\begin{aligned} u_0 = 0, \quad \dot{u}_0 = 0, \\ u_9 = 0, \quad \dot{u}_9 = 0. \end{aligned} \tag{3}$$

Parameters are listed in Table 2.

The experimental setup is shown in Fig. 2. The displacement of each cantilever, $u_n$, is measured by using a strain gauge and bridge circuit. The EM is excited by the current through the current amplifier, which input is fed by the voltage-current converter and the D/A converter. The voice coil motor is individually driven by sinusoidal voltage signal generated by a function generator.

Table 1

Size of cantilever array

| | | | |
|---|---|---|---|
| Length | 70.0 mm | Width | 5.0 mm |
| Thickness | 0.3 mm | Pitch | 15.0 mm |
| Density | $8.0 \times 10^3$ kg/m$^3$ | Young's modulus | 197 GPa |

Table 2

Parameter settings

| Symbol | Value | Symbol | Value |
|---|---|---|---|
| $\omega_0$ | $2\pi\times35.1$ rad/s | $\gamma$ | 1.5 s$^{-1}$ |
| $C$ | 284 s$^{-2}$ | $\chi_0$ | $4.71 \times 10^{-5}$ m$^3$/s$^2$ |
| $d_0$ | 3.0 mm | $\chi_1$ | $9.14 \times 10^{-3}$ m$^3$/s$^2$A |
| $A$ | 3.0 m/s$^2$ | $\omega$ | $2\pi\times36.1$ rad/s |

## 3 Observation of localized oscillations

### *3.1 Single cantilever*

Restoring force of each cantilever varies in nonlinear because of the nonlinearity of magnetic interaction between PM and EM. Fig. 3 shows the relationship between amplitude and frequency for $\gamma = 0,\ A = 0$, namely skeleton curves. The curves asymptotically approach to the line of natural frequency of cantilever according to the increase of amplitude. Because the effect of magnetic interaction decreases as the amplitude becomes large against diameter of the EM. The frequency at small amplitude strongly depends on the current flowing in the EM. The linearization of Eq. (2) gives a resonant frequency

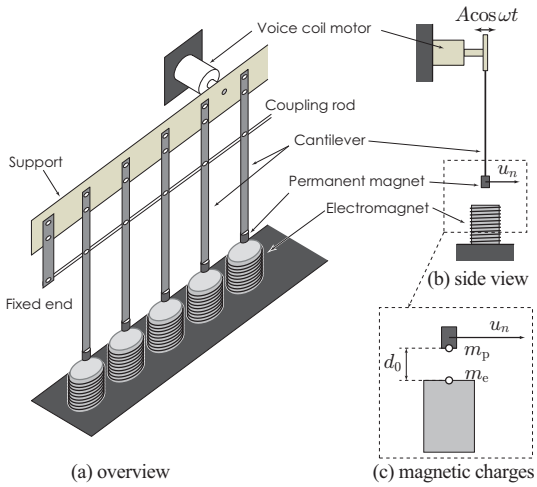


Fig. 1. Schematic configuration of cantilever array. (a) Overview of the cantilever array. Eight cantilevers are mechanically coupled by a coupling rod. The voice coil motor vibrates the cantilever array. (b) Side view of a cantilever. A permanent magnet is attached at the apex of the cantilever. An electromagnet is placed below the permanent magnet. (c) Definition of magnetic charges.

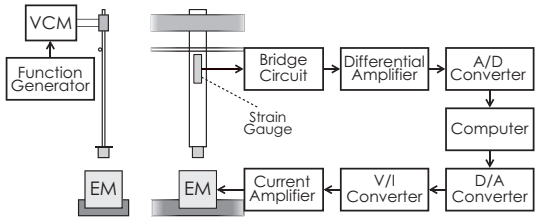


Fig. 2. Experimental setup.

$\omega_0' = \sqrt{\omega_0^2 - (\chi_0 + \chi_1 I_{\mathrm{EM}})/d_0^3}$. In this letter, $\chi_0$ and $\chi_1$ are negative. Thus, the resonant frequency shifts to the high frequency side as the current increases. The curvature of the skeleton curves shows a soft-spring characteristic.

Experimental frequency responses clearly show a hysteresis response against the external force as shown as Fig. 4. The amplitude of a cantilever rapidly increased at 38.3 Hz in the up-scan. However, in the down-scan, the amplitude jumped down at 35.9 Hz. It implies that the single cantilever has two stable states for 35.9 Hz $< \omega/2\pi <$ 38.3 Hz. To excite a localized oscillation, the

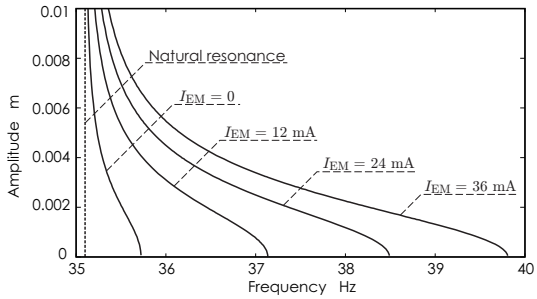


Fig. 3. Skeleton curves. Each curve is obtained numerically.

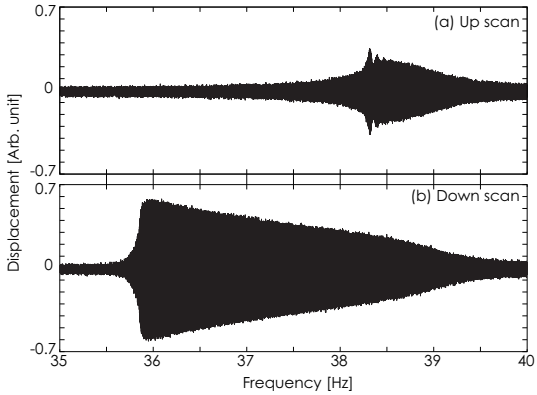


Fig. 4. Frequency response for $I_{\mathrm{EM}} = 24$ mA. (a) Up scan. (b) Down scan. The scan rate was set at 0.05 Hz/s. The damping and external force are estimated to be $\gamma = 1.5$ s$^{-1}$ and $A = 3.0$ m/s$^2$, respectively.

external excitor should be vibrated at a frequency during the hysteric region. On the basis of the analysis, the frequency is set at 36.1 Hz.

### *3.2 Localized oscillations*

Several ILMs ware observed in the coupled cantilever array by external vibration. Figs. 5(a), (b), and (c) show wave forms of observed ILMs. One of arrayed cantilevers has quite large amplitude with respect to the others. Amplitude distribution obviously shows the localization.

We also observed ILMs centered at $n = 2$ and $n = 4$. However, an ILM

standing at $n = 3$ could not be excited because of a disorder. The disorder is implied by a symmetry of amplitude distribution. As shown in Fig. 5(a), amplitude of 6th cantilever is larger than 4th cantilever. That is, the symmetry is slightly broken. Because simulated ILMs in the homogeneous array maintain the symmetry(see Figs. 6(a), (b), and (c)), the symmetry braking will be a cause of the disorder. The fixed boundaries of array can also be considered as impurities. So ILMs standing at $n = 1$ and $n = 8$ were not observed experimentally.

## 4 Conclusion

In this letter, the macro-mechanical cantilever array was proposed for the analysis of ILMs and the model was obtained. The system is analogous to the previous micro- and nano-cantilever array which shows ILMs. In the proposed system, electro magnets placed below cantilevers are tunable and give a soft-spring characteristic. That is, it was experimentally confirmed that the nonlinearity is adjustable by current flowing in EMs.

In experiments, several ILMs were observed experimentally. It implies that ILM can be studied in a macroscopic cantilever arrays. The existence was also confirmed in numerical simulation of the obtained experimental model. Therefore, we can conclude that the proposed cantilever array seems suitable for the study of ILM as same as other experimental systems with precise model. Based on the results, it is possible to study the manipulation of ILM using localized impurity, which can be introduced by EM. The proposed cantilever array will contribute to the forth coming discussion on control of ILM.

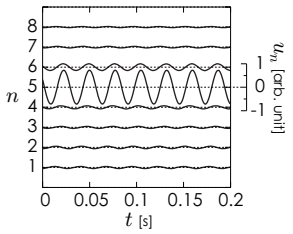


(a) ILM at $n = 5$

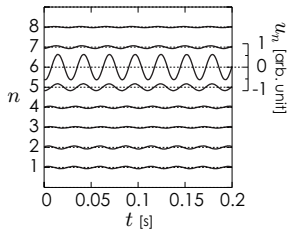


(b) ILM at $n = 6$

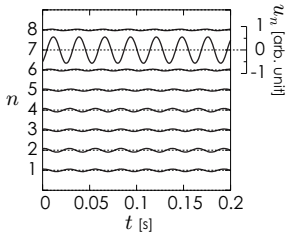


(c) ILM at $n = 7$

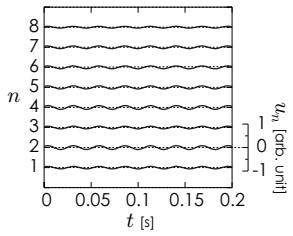


(d) No ILM

Fig. 5. Experimentally excited ILMs. An ILM was excited at $n = 5$ (a), $n = 6$ (b), and $n = 7$ (c). It was also observed that there was no ILM (d).

**Acknowledgements**

We would like to show our appreciation to Professor M. Sato, Kanazawa University, Japan, for the discussion about the model of cantilever array. This research was partially supported by the Ministry of Education, Culture, Sports, Science and Technology in Japan, The 21st Century COE Program No. 14213201 and the Global-COE program.

**References**

[1] S. Flach, C. R. Willis, Discrete breathers, Phys. Rep. 295 (1998) 181.

[2] A. J. Sievers, S. Takeno, Intrinsic localized modes in anharmonic crystals, Phys.

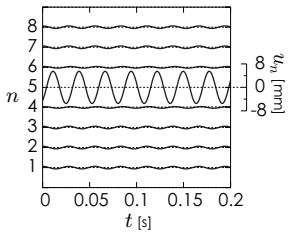


(a) ILM at $n = 5$

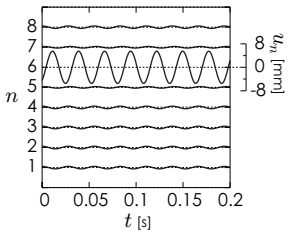


(b) ILM at $n = 5$

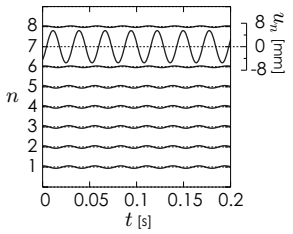


(c) ILM at $n = 5$

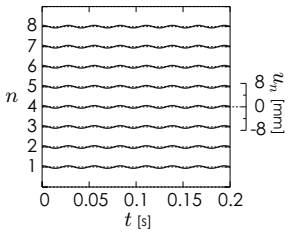


(d) No ILM

Fig. 6. Numerically obtained ILMs for Eq. (2).

Rev. Lett. 61 (1988) 970.

[3] E. Trías, J. J. Mazo, T. P. Orlando, Discrete breathers in nonlinear lattices: Experimental detection in a josephson array, Phys. Rev. Lett. 84 (2000) 741.

[4] P. Binder, D. Abraimov, A. V. Ustinov, S. Flach, Y. Zolotaryuk, Observation of breathers in josephson ladders, Phys. Rev. Lett. 84 (2000) 745.

[5] A. V. Ustinov, Imaging of discrete breathers, Chaos 13 (2003) 716.

[6] H. S. Eisenberg, Y. Silberberg, R. Morandotti, A. R. Boyd, J. S. Aitchison, Discrete spatial optical solitons in waveguide arrays, Phys. Rev. Lett. 81 (1998) 3383.

[7] R. Morandotti, U. Peschel, J. S. Aitchison, H. S. Eisenberg, Y. Silberberg, Dynamics of discrete solitons in optical waveguide arrays, Phys. Rev. Lett. 83 (1999) 2726.

[8] J. W. Fleischer, M. Segev, N. K. Efremidis, D. N. Christodoulides, Observation

of two-dimensional discrete solitons in optically induced nonlinear photonic lattices, Nature 422 (2003) 147.

[9] M. Sato, B. E. Hubbard, A. J. Sievers, B. Ilic, D. A. Czaplewski, H. G. Craighead, Observation of locked intrinsic localized vibrational modes in a micromechanical oscillator array, Phys. Rev. Lett. 90 (2003) 044102.

[10] B. I. Swanson, J. A. Brozik, S. P. Love, G. F. Strouse, A. P. Shreve, A. R. Bishop, W.-Z. Wang, M. I. Salkola, Observation of intrinsically localized modes in a discrete low-dimensional material, Phys. Rev. Lett. 82 (1999) 3288.

[11] K. Kisoda, N. Kimura, H. Harima, K. Takenouchi, M. Nakajima, Intrinsic localized vibrational modes in a highly nonlinear halogen-bridged metal, J. Lumin. 94 (2001) 743.

[12] M. Sato, A. J. Sievers, Direct observation of the discrete character of intrinsic localized modes in an antiferromagnet, Nature 432 (2004) 486.

[13] M. Sato, S. Yasui, M. Kimura, T. Hikihara, A. J. Sievers, Management of localized energy in discrete nonlinear transmission lines, Europhys. Lett. 80 (2007) 30002.

[14] P. S. Waggoner, H. G. Craighead, Micro- and nanomechanical sensors for environmental, chemical, and biological detection, Lab Chip 7 (2007) 1238.

[15] M. Sato, B. E. Hubbard, A. J. Sievers, B. Ilic, H. G. Craighead, Optical manipulation of intrinsic localized vibrational energy in cantilever arrays, Europhys. Lett. 66 (3) (2004) 318.

[16] M. Sato, B. E. Hubbard, A. J. Sievers, *Colloquium:* nonlinear energy localization and its manipulation in micromechanical oscillator arrays, Rev. Mod. Phys. 78 (2006) 137.

[17] T. Hikihara, Y. Okamoto, Y. Ueda, An experimental spatio-temporal state transition of coupled magneto-elastic system, Chaos 7 (1997) 810.

[18] T. Hikihara, K. Torii, Y. Ueda, Wave and basin structure in spatially coupled magneto-elastic beam system – transitions between coexisting wave solutions, Int. J. Bifurcat. and Chaos 11 (2001) 999.

[19] T. Hikihara, K. Torii, Y. Ueda, Quasi-periodic wave and its bifurcation in coupled magneto-elastic beam system, Phys. Lett. A 281 (2001) 155.